



# Human disturbance increases trophic niche overlap in terrestrial carnivore communities

Philip J. Manlick<sup>a,b,1</sup>  and Jonathan N. Pauli<sup>a</sup>

<sup>a</sup>Department of Forest and Wildlife Ecology, University of Wisconsin–Madison, Madison, WI 53706; and <sup>b</sup>Biology Department, University of New Mexico, Albuquerque, NM 87131

Edited by Rodolfo Dirzo, Stanford University, Stanford, CA, and approved August 29, 2020 (received for review June 24, 2020)

**Animal foraging and competition are defined by the partitioning of three primary niche axes: space, time, and resources. Human disturbance is rapidly altering the spatial and temporal niches of animals, but the impact of humans on resource consumption and partitioning—arguably the most important niche axis—is poorly understood. We assessed resource consumption and trophic niche partitioning as a function of human disturbance at the individual, population, and community levels using stable isotope analysis of 684 carnivores from seven communities in North America. We detected significant responses to human disturbance at all three levels of biological organization: individual carnivores consumed more human food subsidies in disturbed landscapes, leading to significant increases in trophic niche width and trophic niche overlap among species ranging from mesocarnivores to apex predators. Trophic niche partitioning is the primary mechanism regulating coexistence in many communities, and our results indicate that humans fundamentally alter resource niches and competitive interactions among terrestrial consumers. Among carnivores, niche overlap can trigger interspecific competition and intraguild predation, while the consumption of human foods significantly increases human–carnivore conflict. Our results suggest that human disturbances, especially in the form of food subsidies, may threaten carnivores by increasing the probability of both interspecific competition and human–carnivore conflict. Ultimately, these findings illustrate a potential decoupling of predator–prey dynamics, with impacts likely cascading to populations, communities, and ecosystems.**

competition | food subsidies | niche overlap | stable isotopes

**E**cological theory posits that organisms must limit niche overlap by partitioning space, time, or resources to coexist (1–3). Niche partitioning in turn promotes biodiversity and is critical to ecosystem functioning and stability (2, 4). However, human disturbance is restructuring terrestrial ecosystems with global consequences for niche dynamics and biotic interactions (5, 6). For example, expanding human footprints have reduced the available niche space for mammals in two of the three primary niche dimensions by restricting animal movements in space (7) and limiting temporal partitioning through increased wildlife nocturnality (8). Human disturbance can similarly transform resource niches and prey partitioning with widespread consequences for population, community, and ecosystem dynamics (9–12). The effect of human disturbance on mammalian resource use and trophic niches, however, has been largely restricted to single species or local scales, and trophic niche dynamics across communities remain undetermined (13).

Humans have systematically extirpated apex predators, disrupting trophic interactions, food web dynamics, and ecological processes across ecosystems (6, 14, 15). Reestablishing trophic complexity is now a global conservation priority (16–18), and the restoration of mammalian carnivores to modified landscapes has been advocated to restore top-down forces and ecosystem function (14, 18). However, maintaining functional carnivore guilds in such landscapes is challenging due to shifting resource niches and novel trophic interactions. For example, human disturbances often alter resource availability or provide novel food subsidies that can shift trophic niches (11), restructure predator–prey relationships

(19), and increase interspecific competition or human–carnivore conflict (10, 13, 20, 21). Shifting trophic niches are likely to have particularly strong impacts on carnivore communities, given that trophic niche partitioning is the primary mechanism regulating competition and interspecific killing (22). Quantifying the influence of humans on resource partitioning and trophic interactions is therefore critical to understanding both the ecological and societal impact of carnivores in the Anthropocene.

We quantified the effect of human disturbance on trophic interactions and niche partitioning using stable isotope analysis ( $\delta^{13}\text{C}$  and  $\delta^{15}\text{N}$ ) of 684 individuals from seven communities along a gradient of human disturbance featuring seven sympatric apex and mesocarnivores (gray wolves [*Canis lupis*; hereafter, wolves], coyotes [*Canis latrans*], bobcats [*Lynx rufus*], red foxes [*Vulpes vulpes*], gray foxes [*Urocyon cinereoargenteus*], fishers [*Pekania pennanti*], and American martens [*Martes americana*; hereafter, martens]) (Fig. 1 and *SI Appendix, Tables S1 and S2*). Stable isotope baselines vary across broad spatial scales (23), so we restricted our analysis to sites within the temperate broadleaf and mixed forest biome of the Great Lakes region in the eastern United States (24). One of the most altered biomes on the planet (25), this region is notable for its recovered carnivore communities, high carnivore richness, and broad spectrum of human disturbance—our sites ranged from protected national parks to urban and exurban landscapes. Moreover, the region is defined by  $\text{C}_3$  primary production, enabling the assessment of human food consumption by carnivores via  $\delta^{13}\text{C}$  analysis (26, 27). We modeled trophic structure as a function of human footprint index (28) at

## Significance

**Niche theory posits that species must limit overlap in the use of space, time, or resources to minimize competition. However, human disturbances are rapidly altering ecosystems with uncertain consequences for niche partitioning. Dietary niche partitioning is the primary way many species limit interspecific competition, and it is particularly important for carnivores because diet overlap can trigger interference competition and interspecific killing. We used stable isotope analyses to examine carnivore diets across the Great Lakes region in the United States and show that carnivores inhabiting disturbed ecosystems consume more human foods, leading to significant increases in both niche breadth and dietary niche overlap among competing species. These results suggest that carnivores in human-dominated landscapes experience significant interspecific competition and conflict due to the consumption of human food subsidies.**

Author contributions: P.J.M. and J.N.P. designed research; P.J.M. performed research; P.J.M. analyzed data; and P.J.M. and J.N.P. wrote the paper.

The authors declare no competing interest.

This article is a PNAS Direct Submission.

Published under the [PNAS license](#).

<sup>1</sup>To whom correspondence may be addressed. Email: pmanlick@unm.edu.

This article contains supporting information online at <https://www.pnas.org/lookup/suppl/doi:10.1073/pnas.2012774117/-DCSupplemental>.

three biological levels: individuals, populations, and communities. We used Bayesian hierarchical mixed effects models to quantify responses in individual consumption of human foods ( $\delta^{13}\text{C}$ ,  $\delta^{15}\text{N}$ ; per mille, ‰), trophic niche width per population (SEAC; ‰), and pairwise trophic niche overlap between species within each community ( $O$ ; ‰). Models accounted for covariates known to influence trophic and isotopic niches, including sample size, spatial extent, community richness, and body mass. For each response variable, we developed a suite of a priori models (SI Appendix, Tables S3–S6), identified top models using leave-one-out cross-validation (29), and interpreted effect sizes to assess the influence of human disturbance on trophic niches. In addition, we estimated the proportional consumption of human food subsidies by each species as a function of human disturbance using stable isotope mixing models.

Increasing evidence suggests carnivores are adaptable foragers that consume human resource subsidies, like refuse or agricultural residuals, as well as novel prey-like domestic animals and synanthropic wildlife (12, 26, 30). However, the consequences of this dynamic foraging for biotic interactions like competition and niche partitioning have been underexplored at the community level. We predicted that individual carnivores would consume more human resource subsidies in disturbed ecosystems (i.e.,  $\delta^{13}\text{C}$ ,  $\delta^{15}\text{N}$  values would increase), leading to trophic niche expansion at the population level. Furthermore, we predicted that this niche expansion would precipitate increased niche overlap among competing carnivores in disturbed landscapes.

## Results and Discussion

We found a strong and consistent response to human disturbance— $\delta^{13}\text{C}$ ,  $\delta^{15}\text{N}$ , niche width, and niche overlap all increased with human footprint (SI Appendix, Tables S1–S5). At the individual level,  $\delta^{13}\text{C}$  (median  $\beta = 0.13$ ; 95% credible interval = 0.02 to 0.24) and  $\delta^{15}\text{N}$  ( $\beta = 0.03$ , 95% credible interval = -0.02 to 0.08) values increased with human footprint for all sampled carnivores, including apex predators like wolves (Fig. 2). Similarly, we found that the proportional consumption of human foods increased with human footprint, and we estimated that >25% of the average carnivore diet was composed of human foods in the most disturbed landscapes (Fig. 3). These results indicate strong dietary responses to human disturbance at the individual level and suggest substantial use of human resource subsidies by an entire guild of carnivores. Local studies have documented elevated  $\delta^{13}\text{C}$  and  $\delta^{15}\text{N}$  values in carnivores due to the consumption of human resource subsidies (11, 12, 26, 27), with wide-ranging consequences. For example, high use of human food subsidies has been tied to increases in human–carnivore conflict (13, 21, 31, 32) and disease prevalence (20, 33), both with consequences for individual survival. Moreover, consumption of human foods can create ecological traps (32), alter space use (26), and even increase interspecific killing (11, 13) and cannibalism (34). Thus, the observed consumption of human resource subsidies in disturbed landscapes has considerable potential to alter population and community dynamics, and our results suggest these consequences extend across a guild of

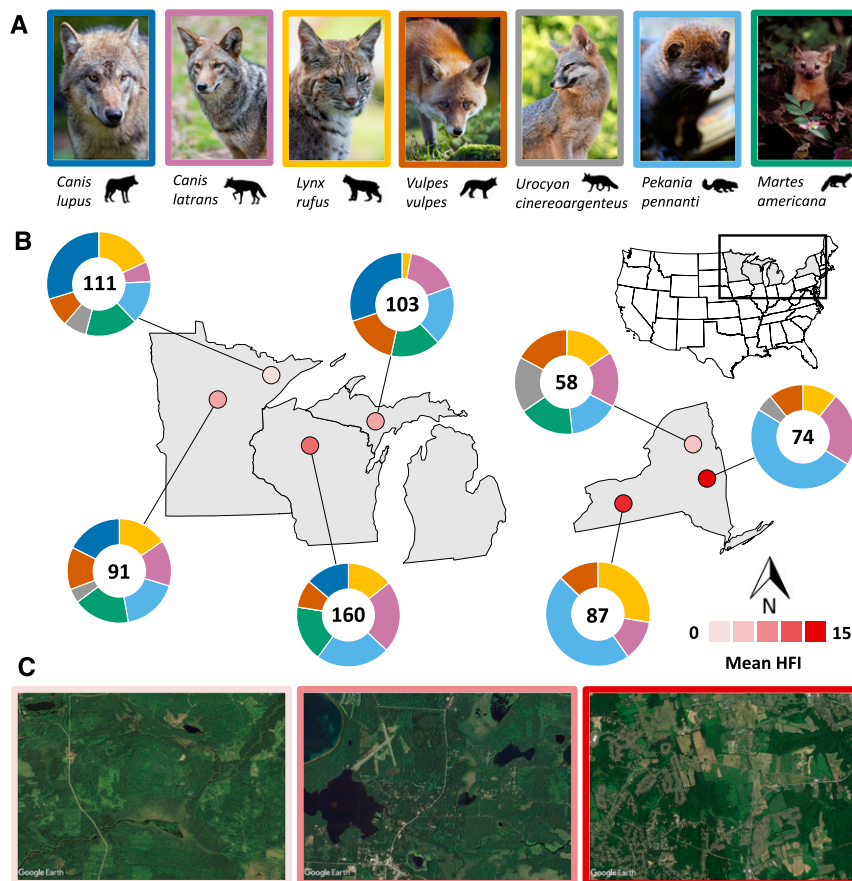


**Fig. 1.** Distribution of carnivores from seven sites across gradient of human footprint index (HFI). (A) Seven competing carnivores in the temperate broadleaf and mixed forest biome ordered by descending body mass and competitive dominance: gray wolves (*C. lupus*; dark blue), coyotes (*C. latrans*; violet), bobcats (*L. rufus*; yellow), red foxes (*V. vulpes*; orange), gray foxes (*U. cinereoargenteus*; gray), fishers (*P. pennanti*; light blue), and American martens (*M. americana*; green). Images credit (Left to Right): Flickr/Tambako the Jaguar/Renee Grayson and Wikimedia Commons/United States National Park Service/United States Fish and Wildlife Service. (B) Donut plots with sample size (in the center) and proportion of species sampled per site; red points illustrate mean HFI per site. (Inset) Map with site locations. (C) Example landscapes from sites with low (HFI = 3.66; Superior National Forest, MN), medium (HFI = 6.05; Chequamegon-Nicolet National Forest, WI), and high (HFI = 13.20; Albany, NY) human footprints.

widespread carnivores. Nevertheless, we detected substantial plasticity among carnivores, as the average magnitude and response to disturbance varied by species. For instance, bobcats, the only obligate carnivore, exhibited low  $\delta^{13}\text{C}$  values ( $\delta^{13}\text{C}_{\text{Intercept}} = -24.80\text{‰}$ ,  $\beta = 0.16$ ) (Fig. 2A) and consumed minimal human food subsidies even in the most disturbed landscapes (Fig. 3D). Conversely, dietary generalists like red foxes had elevated  $\delta^{13}\text{C}$  values ( $\delta^{13}\text{C}_{\text{Intercept}} = -22.72\text{‰}$ ,  $\beta = 0.10$ ) (Fig. 2A), with an estimated 50% of their diet composed of human foods in highly disturbed landscapes (Fig. 3E).

SEAc also increased as a function of human footprint ( $\beta = 0.93$ , 95% credible interval = 0.02 to 1.80) for all carnivores, but average niche width varied by species (Fig. 4A and B). This trophic niche expansion indicates a broader incorporation of dietary resources by carnivores in human-dominated landscapes, likely via consumption of human refuse or domestic and synanthropic wildlife subsidized by C4 plants (11, 18, 26) (Fig. 3). Indeed, human population density, a strong proxy for food subsidies (35), significantly influenced all trophic metrics (SI Appendix, Table S5), indicating that the observed niche expansion was a function of human food consumption, not variation in baseline carbon sources. In addition to human footprint, we detected a strong relationship between SEAc and carnivore richness ( $\beta = 2.10$ , 95% credible interval = 0.32 to 3.97) but little effect of sample size ( $\beta = -0.09$ , 95% credible interval =  $-0.37$  to 0.20). While carnivore richness and competition can structure foraging (30), richness was strongly correlated with site area, a known driver of isotopic niche width (23). Consequently, the apparent influence of carnivore richness is likely conflated with site area and represents underlying isotopic variability in the landscape. Nevertheless, our top model accounted for these differences and still detected trophic niche expansion, suggesting strong dietary plasticity and adaptability across this carnivore guild.

Trophic niche overlap between carnivore species increased significantly with human footprint ( $\beta = 0.07$ , 95% credible interval = 0.01 to 0.13) (Fig. 4C and D); however, overlap varied across species in predictable ways. Generalists like red foxes ( $\beta_0^{\text{offset}} = 0.39$ ) and coyotes ( $\beta_0^{\text{offset}} = 0.33$ ) exhibited high overlap with competitors, likely due to trophic plasticity and niche expansion (Fig. 4C). In contrast, obligate carnivores like bobcats—felids with specialized dentition—exhibited the highest degree of trophic niche overlap ( $\beta_0^{\text{offset}} = 0.94$ ) (Fig. 4C), presumably due to limited trophic flexibility (e.g., Fig. 3D). Smaller carnivores like martens ( $\beta_0^{\text{offset}} = -0.27$ ) and gray foxes ( $\beta_0^{\text{offset}} = -0.69$ ) exhibited the least niche overlap (Fig. 4C), suggesting these competitively subordinate species may shift their realized trophic niches entirely to minimize competitive overlap. We also detected a significant influence of carnivore richness on niche overlap ( $\beta = 0.20$ , 95% credible interval = 0.09 to 0.32) (Fig. 4C). However, richness was again correlated with site area, indicating that this effect is likely a combination of isotopic variation and diffuse competition within diverse carnivore communities (36). Importantly, the total niche width of the community did not increase with human disturbance ( $P = 0.32$ ), indicating that while niche overlap and competition increased in human-dominated landscapes, the overall available niche space was consistent across sites.

We found that the consumption of human foods increased SEAc and niche overlap across carnivores. However, it is possible that the consumption of native prey subsidized by agriculture (e.g., corn) could have contributed to this effect. We estimated the proportional consumption of natural vs. human foods across a disturbance gradient and found that most carnivore species consumed substantially higher proportions of human foods in disturbed landscapes (Fig. 3). If native prey were subsidized by agriculture, they would be isotopically indiscernible from human food subsidies, and we would expect all carnivore species to exhibit increased human foods in their diet. This was not the case. Rather, we found that bobcats—our only obligate carnivore—

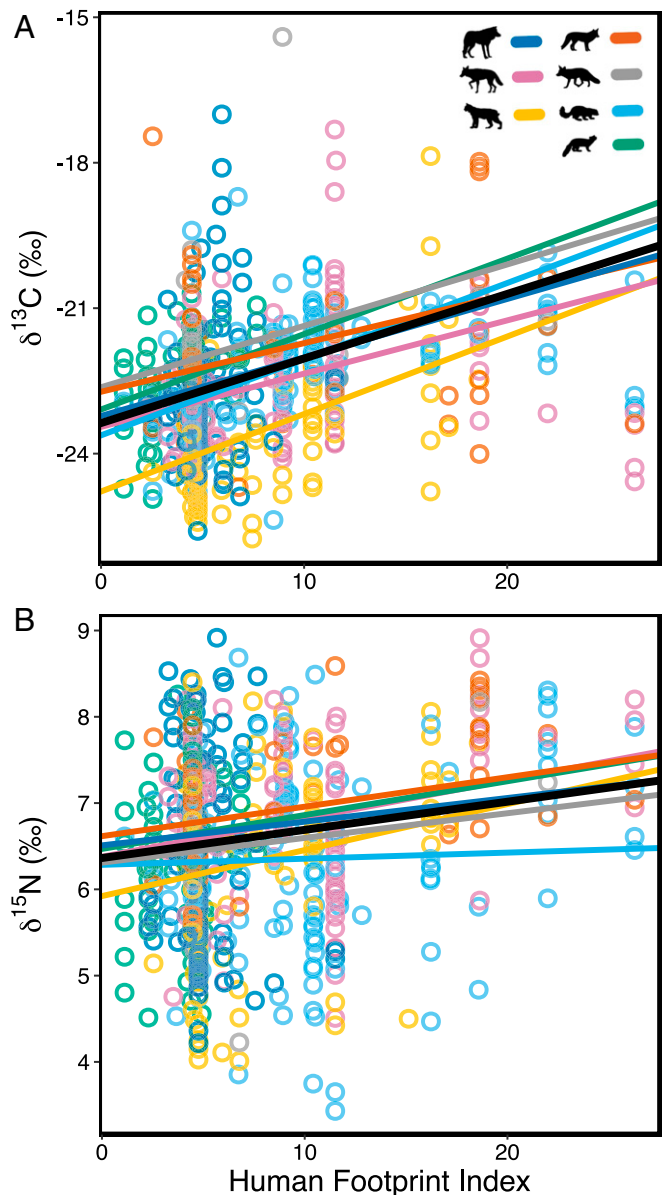


**Fig. 2.** Individual responses to human footprint index. Response of  $\delta^{13}\text{C}$  (A) and  $\delta^{15}\text{N}$  (B) values to human footprint for gray wolves (*C. lupus*; dark blue), coyotes (*C. latrans*; violet), bobcats (*L. rufus*; yellow), red foxes (*V. vulpes*; orange), gray foxes (*U. cinereoargenteus*; gray), fishers (*P. pennanti*; light blue), and American martens (*M. americana*; green). Black lines indicate global mean response to human footprint. All lines represent median slopes and intercepts from Bayesian mixed effects models.

consumed <5% human foods across sites, while wolves exhibited a similarly attenuated response (Fig. 3). This suggests that generalist species with high proportions of human foods in their diet (e.g., coyotes and foxes) consumed these subsidies directly, while apex predators (e.g., wolves) and specialized carnivores with limited dietary plasticity (e.g., bobcats) largely maintained their foraging niches. Ultimately, the observed trophic signal is likely a combination of both direct consumption of human foods and the subsidization of local prey, but these results clearly illustrate the pervasive impact of human subsidies on terrestrial food webs.

## Conclusions

We found that human disturbance is altering carnivore foraging and resource use, leading to trophic niche expansion and trophic

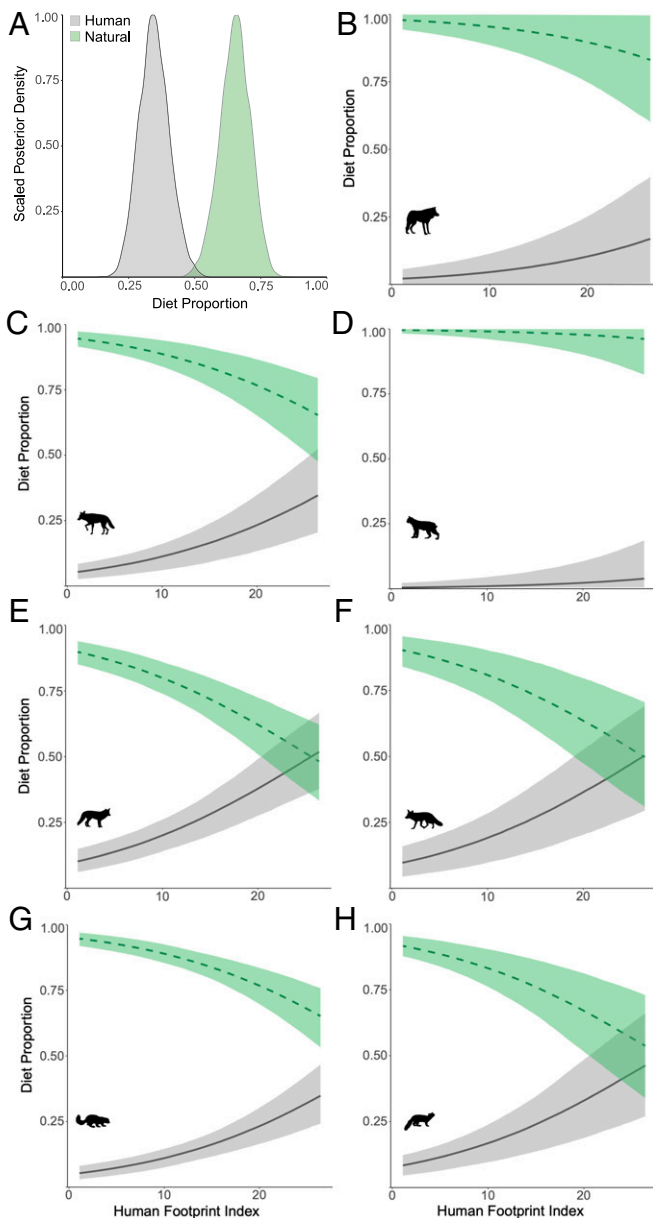


**Fig. 3.** Proportional use of human (gray; solid lines) and natural (green; dashed lines) prey by individual carnivores as a function of human footprint index. (A) Estimated diet of the average carnivore at maximum observed human footprint and the proportional consumption of human and natural foods by gray wolves (*C. lupis*; B), coyotes (*C. latrans*; C), bobcats (*L. rufus*; D), red foxes (*V. vulpes*; E), gray foxes (*U. cinereoargenteus*; F), fishers (*P. pennanti*; G), and martens (*M. americana*; H).

niche overlap across a widespread guild of North American carnivores. It is important to note that while we found extensive trophic niche overlap, carnivores could still partition space and time to minimize competitive interactions. However, human disturbance has already severely reduced the spatial and temporal niches of animals (7, 8), likely exacerbating the consequences of trophic niche overlap (10). Our results also show that human subsidies pervade terrestrial food webs and that human disturbance impacts trophic interactions at multiple levels of biological organization. These dynamics will likely impact carnivore populations, communities, and even ecosystems. For example, while the consumption of food subsidies can increase carnivore abundance, it also increases the probability of human–carnivore conflict

(13, 20, 21). Given the continued expansion of human activities, our data suggest human–carnivore conflict will only increase in the Anthropocene, with likely consequences for coexistence and the viability of many carnivore populations. We also found that human disturbance increases dietary overlap but not available niche space, thus increasing the probability of interspecific competition and intraguild predation in human-dominated landscapes (22). Indeed, trophic niche partitioning has preceded the evolution of morphological and dietary divergence within carnivore guilds (37), but expanding trophic niches in human-dominated landscapes could undermine these selective forces that have facilitated coexistence for millennia. Lastly, we observed highly plastic foraging and widespread consumption of human foods, particularly among generalist mesocarnivores (e.g., coyotes and foxes). Mesocarnivores represent the most abundant and diverse group of carnivores—both in our study and globally—and they often perform critical ecological functions through top-down forces (38–40). The observed consumption of human foods could reinforce this top-down suppression (13), or it could decouple predator–prey interactions entirely (41). Ultimately, if carnivores and other mammals are unable to partition space, time, or resources, then conflict—with humans and within communities—is likely to accelerate in the Anthropocene, with cascading effects on populations, communities, and ecosystems.

## Methods

**Sites and Samples.** We quantified the influence of human disturbance on carnivore trophic structure via hierarchical sampling of carnivore species across seven sites in the Great Lakes region (Fig. 1 and *SI Appendix*, Fig. S1). Sites and populations were defined using state-level furbearer management units (*SI Appendix*, Table S7), and communities were defined by carnivore populations that co-occur within a management unit. We quantified human disturbance as the mean human footprint index (28) per site. The human footprint index incorporated multiple aspects of disturbance, including agricultural and developed land, roads and railways, human population density, and nighttime lights (28). In total, sites ranged across a >3.5-fold increase in human disturbance (*SI Appendix*, Table S6). Within each site, we collected biological samples (hair and/or bone) of carnivores for stable isotope analysis via direct sampling of carnivore tissues (e.g., trapper harvest, depredation harvest, collared animals, known-fate mortality) or archived biological collections, and we supplemented sampling with published isotopic values from the literature (42–45) (*SI Appendix*, Table S2). In total, we sampled seven competing carnivore species: gray wolves (*C. lupis*;  $N = 102$ ), coyotes (*C. latrans*;  $N = 111$ ), bobcats (*L. rufus*;  $N = 101$ ), red foxes (*V. vulpes*;  $N = 82$ ), gray foxes (*U. cinereoargenteus*;  $N = 26$ ), fishers (*P. pennanti*;  $N = 174$ ), and American martens (*M. americana*;  $N = 88$ ). Sites varied in community composition and sample sizes (Fig. 1 and *SI Appendix*, Table S7). For all samples, we identified harvest or sampling location to the finest resolution possible (e.g., county, township, management unit), and we recorded harvest date and sex when available (*SI Appendix*, Table S7) (archived data at doi:10.6084/m9.figshare.8006750).

**Stable Isotope Analyses.** We quantified carnivore trophic structure using  $\delta^{13}\text{C}$  and  $\delta^{15}\text{N}$  stable isotope analyses. Stable isotopes in animal tissues reflect the flow of energy through communities, with  $\delta^{13}\text{C}$  capturing the diversity of basal resources in a system and  $\delta^{15}\text{N}$  describing trophic position (46). Patterns in consumer stable isotope values (e.g.,  $\delta^{13}\text{C}$  and  $\delta^{15}\text{N}$ ) allow for the multidimensional quantification of habitat and resource use known as the isotopic or trophic niche (47, 48). Accordingly, stable isotope analyses have become a common tool to quantify the impact of human disturbance on trophic interactions and consumer niche dynamics (11, 26, 49, 50).

We used hair and bone samples to quantify the trophic niches of carnivores across study sites. Hair samples were rinsed three times with a 2:1 chloroform-methanol solution to remove surface contaminants before being homogenized and dried for 72 h at 56 °C. Bone samples were demineralized in 0.5 N hydrochloric acid at 4 °C for a minimum of 24 h, and the remaining bone collagen was lipid extracted via immersion in 2:1 chloroform-methanol solution for a minimum of 72 h. Bone collagen samples were then rinsed with deionized water to remove solvents, dried for 72 h at 56 °C, and homogenized with either a ball mill mixer or mortar and pestle. All samples were weighed into tin capsules for  $\delta^{13}\text{C}$  and  $\delta^{15}\text{N}$  analysis at the University of New Mexico Center for Stable Isotopes using a Costech 4010 elemental analyzer (Costech) coupled to a Thermo Scientific Delta V mass spectrometer (Thermo Scientific).

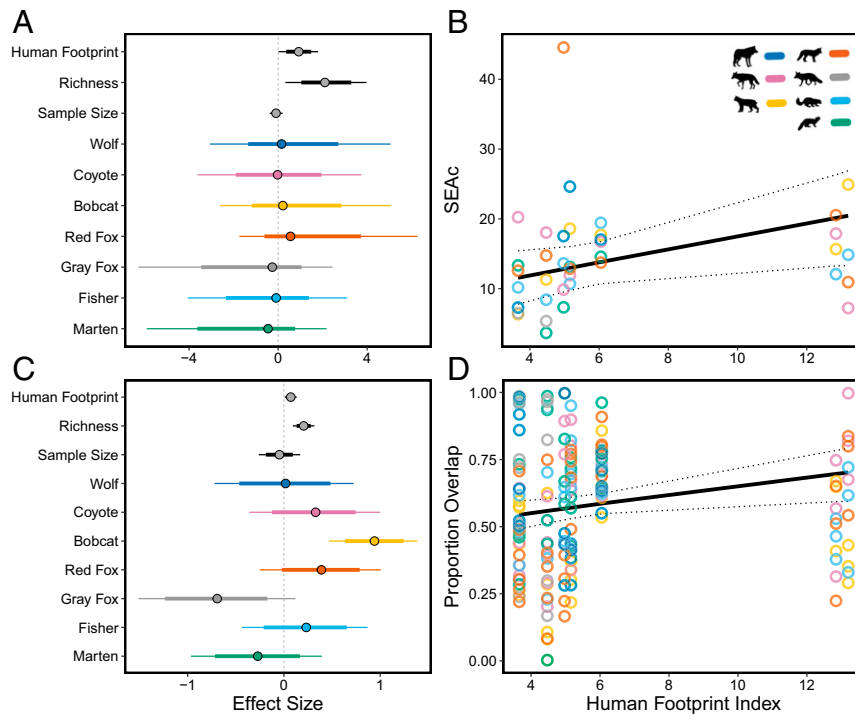


**Fig. 4.** Population and community responses to human footprint index. (A) Effect sizes for top Bayesian mixed effects model of SEAc, including fixed (regression coefficients; black) and random effects (intercept offset; color by species). Thick bars indicate 80% credible intervals, and thin lines indicate 95% credible intervals. (B) Predicted response of SEAc to human footprint across species. The black line indicates median response, dotted lines denote 95% credible intervals, and circles represent SEAc per species per site. (C) Effect sizes for top Bayesian mixed effects model of pairwise niche overlap, including fixed (regression coefficients; black) and random effects (intercept offset; color by species). Thick bars indicate 80% credible intervals, and thin lines indicate 95% credible intervals. (D) Predicted response of pairwise niche overlap to human footprint across species. The black line indicates median response, dotted lines denote 95% credible intervals, and circles represent pairwise overlap ( $O_{ij}$ ) for co-occurring carnivores within each site.

Isotopic ratios were quantified as parts per mille (‰) relative to the international standards Vienna Pee Dee Belemnite (C) and atmospheric nitrogen (N).

Hair is a metabolically inert tissue and reflects the assimilated diet of an individual over the temporal period that the hair was synthesized (51). All harvested and noninvasively collected samples were acquired after the annual molt (approximately June to October) during fall and winter trapping seasons (SI Appendix, Table S7); therefore, all isotopic signatures from hair represent trophic relationships from late summer through fall. Conversely, bone collagen integrates continuously, represents multiple years of assimilated diet, and turns over at a different rate, potentially resulting in divergent isotopic signatures between hair and bone collagen within a single individual (52). We used bone collagen from gray wolf museum specimens to capture the trophic niche of wolves at one site (SI Appendix, Table S7), but we detected no significant differences between paired bone collagen and hair samples using two independent datasets (SI Appendix, Table S8). Thus, all bone collagen isotopic signatures were retained in downstream analyses.

**Trophic Niche Dynamics.** For consumers, the trophic niche defined by  $\delta^{13}\text{C}$  and  $\delta^{15}\text{N}$  values ultimately represents the consumption of prey and the potential impact of a species on its community or environment (i.e., the Eltonian niche) (30). Consequently, shifts in consumer trophic niches largely reflect either niche collapse due to limited prey availability (45, 49) or niche expansion following increased food subsidies (11, 26). Human disturbance has been shown to drastically increase food subsidies (31, 35), with likely consequences for community trophic structure. To assess the impact of human disturbance on carnivore trophic structure, we used Bayesian hierarchical mixed effects models and a leave-one-out model selection framework to analyze stable isotope signatures at three levels: individuals, populations, and communities.

**Individuals.** To quantify individual responses to human disturbance, we subset our data to include all individuals with a known county of origin ( $n = 596$ ), calculated mean human footprint per county, and modeled  $\delta^{13}\text{C}$  and  $\delta^{15}\text{N}$  values as a function of human footprint. We developed a suite of 10 a priori models incorporating site and species as random effects (SI Appendix, Tables

S3 and S4), including a fully varying model with random slopes and intercepts for both site and species, two null models varying only by site or species (i.e., “intercept only”), and all subsets in between. All site-level random effects included a nested county grouping to account for repeated measures within sites. In all of our study sites,  $\text{C}_3$  photosynthetic plants predominate and are easily distinguishable via  $\delta^{13}\text{C}$  values (−28 to −22‰) (26, 53). Conversely, human food subsidies in the United States, including agricultural residuals and human refuse, are largely defined by  $\text{C}_4$  photosynthetic plants like corn (27, 54) with distinct  $\delta^{13}\text{C}$  signatures (−12 to −14‰) (53) that permeate terrestrial food webs via animal consumption (21, 31, 55). Similarly, domestic animals and synanthropic wildlife commonly found in urban carnivore diets also exhibit elevated  $\delta^{15}\text{N}$  values (11, 26). Thus, we predicted that both  $\delta^{13}\text{C}$  and  $\delta^{15}\text{N}$  values would increase with human footprint. To assess the relative impacts of agricultural subsidies vs. human refuse, we ran supplementary analyses using the top model identified during model selection. To assess agricultural inputs likely to influence isotope signatures (e.g., corn), we calculated the proportion of corn planted in each county during the growing season prior to animal harvest using US Department of Agriculture (USDA) Cropland Data Layer Maps ([https://www.nass.usda.gov/Research\\_and\\_Science/Cropland/SARS1a.php](https://www.nass.usda.gov/Research_and_Science/Cropland/SARS1a.php)). To quantify inputs from human refuse, we calculated mean population density per county (humans per square kilometer) in 2010 using the population density layer of the human footprint index (28). Percent corn and population density were significantly correlated ( $r = 0.56$ ,  $P < 0.001$ ). Thus, to assess the influence of corn vs. human refuse, we modeled individual isotopic values as a function of percent corn and population density separately and identified the top model using a leave-one-out model selection framework (SI Appendix, Table S5). We also estimated the proportion of human foods consumed by each individual using Bayesian isotopic mixing models in the R package *mixsiar* (56). Specifically, we used existing stable isotope data on human food subsidies and natural prey (SI Appendix, Table S9) to estimate the proportion of human foods consumed as a function of human footprint, again with a random effect of species. We used trophic discrimination factors of 1.5‰ ( $\pm 0.5$ ) and 3.5‰ ( $\pm 0.5$ ) for  $\delta^{13}\text{C}$  and  $\delta^{15}\text{N}$ , respectively (26). The model used uniform priors with a process  $\times$  residual error structure, and we ran three Markov chains for each model with 100,000

iterations, a 50,000-iteration burn-in, and a thinning rate of 50. Model convergence was identified by Gelman–Rubin diagnostic ( $\hat{R}$ ) values  $< 1.05$ .

**Populations.** To assess species-level responses to human disturbance, we first estimated SEAc for each species at each site (i.e., population;  $n = 38$ ) using 95% standard ellipses corrected for small sample size (SEAc) via the *r* package SIBER (57). We excluded all populations with fewer than five samples ( $\bar{x} = 17.71$ ) following SIBER recommendations (57). We then modeled SEAc (%) for each population as a function of human footprint including species as a random effect. Second, because community composition can also regulate the trophic niches of carnivores (30, 58), we also included carnivore richness as a predictor of SEAc. Carnivore richness was correlated with site area ( $r = 0.88$ ,  $P < 0.001$ ), a strong predictor of isotopic niche width (23), but uncorrelated with human footprint ( $r = -0.11$ ,  $P = 0.49$ ). Thus, we retained carnivore richness to capture both community and scale effects on niche width and denoted richness for each site as the total number of terrestrial carnivore species (order Carnivora) present, as estimated by local natural resource agencies. Despite the unbiased nature of standard ellipses (57), we also included sample size as a predictor of SEAc to account for any potential differences in niche width due to unequal sampling. We developed eight candidate models to test the response of SEAc to human footprint, including a full model with all predictors and species-level responses to human footprint (i.e., random slopes and intercepts), a null model with only a species-level random effect, and subsets with varying predictors and random effect structures (SI Appendix, Table S5). Because both human footprint and carnivore richness are site-level continuous variables, we did not include site as a random effect to minimize covariance within model parameters. We predicted that SEAc would increase with human footprint. We tested the relative impacts of agricultural subsidies vs. human refuse using 2010 population density and the mean proportion of corn planted during the respective sampling window for each site. Percent corn and population density were again significantly correlated ( $r = 0.79$ ,  $P < 0.001$ ). We used the top model from our initial analysis of SEAc, replaced human footprint with percent corn and population density, and modeled SEAc as a function of each variable separately. We then identified the top model using leave-one-out model selection.

**Communities.** We quantified community-level responses to human disturbance by estimating trophic niche overlap between all species pairs within each site ( $n = 176$ ). We estimated niche overlap for each species as

$$O_{ij} = \frac{\sigma_{ij}}{SEAc_i}$$

where  $i$  indicates the species of interest,  $j$  indicates the competing species,  $\sigma_{ij}$  indicates the area of SEAc overlap between competitors (%), and  $SEAc_i$  indicates the total trophic niche area for the species of interest (%). The resultant metric ( $O_{ij}$ ) represents the proportion of a given species' trophic niche overlapped by a potential competitor and ranges from zero (no overlap) to one (complete overlap). We calculated  $O_{ij}$  for both species in all species pairs within each site. We then modeled  $O_{ij}$  as a function of human footprint including species as a random effect to assess differences in trophic niche overlap by species. We again included carnivore richness as a covariate to account for community and scale effects on trophic niches, and we also included the sample size ratio between each species pair to account for potential differences in proportional overlap due to unequal sample sizes. Given that diet overlap in carnivores is often a function of body size difference (BSD), we estimated BSD for all pairwise species comparisons following Donadio and Buskirk (22). For each species, we estimated mean body mass (kilograms) using published values from the literature and cataloged biological specimens on VertNet (SI Appendix, Table S9). All populations and individuals used to estimate body mass were restricted to the Great Lakes region, and we estimated mean body mass for midwestern and northeastern coyotes separately due to the significant differences in body mass between regions (59). In total, we developed a suite of 12 candidate models to quantify the impact of human footprint on pairwise niche overlap, including a full model with all predictors and species-level responses to human footprint (i.e., random slopes and intercepts), a null model with only a species-level random effect, and subsets with varying predictors and random effect structures (SI Appendix, Table S6). Because human footprint and carnivore richness

are site-level continuous variables, we did not include site as a random effect to minimize covariance within model parameters. We predicted that  $O_{ij}$  would increase with human footprint. We tested the relative impacts of agricultural subsidies (i.e., corn) vs. human refuse using population density and the mean proportion of corn planted during the respective sampling window for each site. Corn and population density were again correlated ( $r = 0.79$ ,  $P < 0.001$ ), so we used the top model from our initial analysis, replaced human footprint with percent corn and population density, and modeled  $O_{ij}$  as a function of each variable separately. We used leave-one-out model selection to identify the best-fitting model. Lastly, we calculated the community niche width (i.e., the range of resources available to each community) by combining all carnivores from each site and calculating SEAc. To assess the relationship between human disturbance and total niche width of the community, we used Pearson's correlation and tested for significance using the *cor.test* function in R.

**Statistical Procedures.** All statistical analyses were performed in the statistical software *r* (60). Models were implemented in the *r* package *rstanarm* v. 2.18.2 (61). The *rstanarm* package uses a Hamiltonian Markov chain Monte Carlo sampling algorithm that efficiently samples parameter space to provide robust inferences on ecological processes (62). We used the default, weakly informative priors for all models—normal (0, 10) on intercepts, normal (0, 2.5) on coefficients—and predictors were centered and scaled internally by *rstanarm* to have a mean of zero and SD of one. Models of  $\delta^{13}\text{C}$ ,  $\delta^{15}\text{N}$ , and SEAc held continuous and unbounded response variables and used linear mixed effect regressions with Gaussian likelihood distributions. Conversely,  $O_{ij}$  required a bounded distribution (0, 1), and we therefore used beta-regression with a Beta likelihood distribution and logit link. Beta-regressions do not, however, permit boundary values (0 or 1) which were present in our data. We therefore transformed  $O_{ij}$  data using the equation

$$\frac{y * (n - 1) + 0.5}{n},$$

where  $y$  was the  $O_{ij}$  value and  $n$  was sample size, effectively limiting data to (0.005, 0.995) (63). We set proposal acceptance probability to a minimum of 0.95 (maximum 0.995) to avoid divergent transitions while maximizing model efficiency. Models ran four chains with 2,000 iterations, with the first 1,000 iterations discarded as burn-in. All models exhibited convergence (all  $\hat{R} = 1.0$ ), and effective posterior sample sizes exceeded 1,000 in all cases. We compared multiple models for each analysis by estimating the expected log predictive density (ELPD) for each model using the approximate leave-one-out cross-validation procedure in the *r* package *loo* v. 2.1.0 (29, 64). We used a Pareto  $K$  threshold of 0.7 to account for the impact of potential outliers and selected top models via comparison of ELPD, with top-ranked models exhibiting the highest ELPD values. Lastly, we visually inspected model diagnostics to assess convergence (e.g., trace plots) using the *r* package *shinystan* (65), and we used a series of posterior predictive checks to ensure that 1) models reasonably approximated mean values from the data and 2) all residual errors were zero centered and normal.

**Data Availability.** Data are available in SI Appendix, and stable isotope ratios data can be accessed in full at FigShare, <https://doi.org/10.6084/m9.figshare.8006750.v1>.

**ACKNOWLEDGMENTS.** We thank the many biologists who helped provide samples for this project, including J. Olsen, N. Roberts, and S. Rossler at the Wisconsin Department of Natural Resources; J. Gilbert at the Great Lakes Indian Fish and Wildlife Commission; S. Windels and T. Gable at Voyageurs National Park; J. Erb and N. Hanson at the Minnesota Department of Natural Resources; M. Clark and S. Smith at the New York Division of Environmental Conservation; D. Beyer and A. Bump at the Michigan Department of Natural Resources; K. Galbreath at Northern Michigan University; and P. Holahan at the University of Wisconsin Zoological Museum. We also thank the USDA Animal and Plant Health Inspection Service (APHIS) Wildlife Services, North American Fur Auctions, Groenwald Fur and Wool Company, and all the independent hunters and trappers. This work was supported by NSF Integrative Graduate Education and Research Traineeship (IGERT) Grant DGE-1144752; National Institute of Food and Agriculture, USDA Hatch Projects 1006604 and 1003605; and the University of Wisconsin Department of Forest and Wildlife Ecology, with additional funds provided by the American Society of Mammalogists, the American Museum of Natural History, and the National Park Service.

1. G. Hutchinson, Concluding remarks. *Cold Spring Harbor Symp. Quant. Biol.* **22**, 415–427 (1957).
2. P. Chesson, Mechanisms of maintenance of species diversity. *Annu. Rev. Ecol. Syst.* **31**, 343–358 (2000).

3. R. H. MacArthur, R. Levins, The limiting similarity, convergence, and divergence of coexisting species. *Am. Nat.* **101**, 377–385 (1967).
4. D. Tilman et al., The influence of functional diversity and composition on ecosystem processes. *Science* **277**, 1300–1302 (1997).

5. J. A. Foley *et al.*, Global consequences of land use. *Science* **309**, 570–574 (2005).
6. J. A. Estes *et al.*, Trophic downgrading of planet Earth. *Science* **333**, 301–306 (2011).
7. M. A. Tucker *et al.*, Moving in the Anthropocene: Global reductions in terrestrial mammalian movements. *Science* **359**, 466–469 (2018).
8. K. M. Gaynor, C. E. Hohnowski, N. H. Carter, J. S. Brashares, The influence of human disturbance on wildlife nocturnality. *Science* **360**, 1232–1235 (2018).
9. R. M. Thompson *et al.*, Food webs: Reconciling the structure and function of biodiversity. *Trends Ecol. Evol.* **27**, 689–697 (2012).
10. J. A. Smith, A. C. Thomas, T. Levi, Y. Wang, C. C. Wilmers, Human activity reduces niche partitioning among three widespread mesocarnivores. *Oikos* **127**, 890–901 (2018).
11. W. E. Moss, M. W. Allredge, K. A. Logan, J. N. Pauli, Human expansion precipitates niche expansion for an opportunistic apex predator (*Puma concolor*). *Sci. Rep.* **6**, 39639 (2016).
12. M. Magioli *et al.*, Human-modified landscapes alter mammal resource and habitat use and trophic structure. *Proc. Natl. Acad. Sci. U.S.A.* **116**, 18466–18472 (2019).
13. T. M. Newsome *et al.*, The ecological effects of providing resource subsidies to predators. *Glob. Ecol. Biogeogr.* **24**, 1–11 (2015).
14. W. J. Ripple *et al.*, Status and ecological effects of the world's largest carnivores. *Science* **343**, 1241484 (2014).
15. J. E. Duffy, Biodiversity loss, trophic skew and ecosystem functioning. *Ecol. Lett.* **6**, 680–687 (2003).
16. A. Dobson, S. Allesina, K. Lafferty, M. Pascual, The assembly, collapse and restoration of food webs. *Philos. Trans. R. Soc. Lond. B Biol. Sci.* **364**, 1803–1806 (2009).
17. J. E. Duffy *et al.*, The functional role of biodiversity in ecosystems: Incorporating trophic complexity. *Ecol. Lett.* **10**, 522–538 (2007).
18. A. Perino *et al.*, Rewilding complex ecosystems. *Science* **364**, eaav5570 (2019).
19. J. A. Smith, Y. Wang, C. C. Wilmers, Spatial characteristics of residential development shift large carnivore prey habits. *J. Wildl. Manage.* **80**, 1040–1048 (2016).
20. M. Murray *et al.*, Greater consumption of protein-poor anthropogenic food by urban relative to rural coyotes increases diet breadth and potential for human-wildlife conflict. *Ecography* **38**, 1235–1242 (2015).
21. J. B. Hopkins, P. L. Koch, J. M. Ferguson, S. T. Kalinowski, The changing anthropogenic diets of American black bears over the past century in Yosemite National Park. *Front. Ecol. Environ.* **12**, 107–114 (2014).
22. E. Donadio, S. W. Buskirk, Diet, morphology, and interspecific killing in carnivora. *Am. Nat.* **167**, 524–536 (2006).
23. C. J. Reddin, J. H. Bothwell, N. E. O'Connor, C. Harrod, The effects of spatial scale and isoscape on consumer isotopic niche width. *Funct. Ecol.* **32**, 904–915 (2018).
24. D. M. Olson *et al.*, Terrestrial ecoregions of the world: A new map of life on earth. *Bioscience* **51**, 933–938 (2001).
25. J. M. Hoekstra, T. M. Boucher, T. H. Ricketts, C. Roberts, Confronting a biome crisis: Global disparities of habitat loss and protection. *Ecol. Lett.* **8**, 23–29 (2005).
26. S. D. Newsome, H. M. Garbe, E. C. Wilson, S. D. Gehrt, Individual variation in anthropogenic resource use in an urban carnivore. *Oecologia* **178**, 115–128 (2015).
27. R. Kirby, D. M. Macfarland, J. N. Pauli, Consumption of intentional food subsidies by a hunted carnivore. *J. Wildl. Manage.* **81**, 1161–1169 (2017).
28. O. Venter *et al.*, Sixteen years of change in the global terrestrial human footprint and implications for biodiversity conservation. *Nat. Commun.* **7**, 12558 (2016).
29. A. Vehtari, A. Gelman, J. Gabry, Practical Bayesian model evaluation using leave-one-out cross-validation and WAIC. *Stat. Comput.* **27**, 1413–1432 (2017).
30. P. J. Manlick, S. M. Petersen, K. M. Moriarty, J. N. Pauli, Stable isotopes reveal limited Eltonian niche conservatism across carnivore populations. *Funct. Ecol.* **33**, 335–345 (2019).
31. R. Kirby, M. W. Allredge, J. N. Pauli, The diet of black bears tracks the human footprint across a rapidly developing landscape. *Biol. Conserv.* **200**, 51–59 (2016).
32. W. E. Moss, M. W. Allredge, J. N. Pauli, Quantifying risk and resource use for a large carnivore in an expanding urban-wildland interface. *J. Appl. Ecol.* **53**, 371–378 (2016).
33. M. Murray, M. A. Edwards, B. Abercrombie, C. C. St. Clair, Poor health is associated with use of anthropogenic resources in an urban carnivore. *Proc. Biol. Sci.* **282**, 20150009 (2015).
34. T. M. Newsome, C. Howden, A. J. Wirsing, Restriction of anthropogenic foods alters a top predator's diet and intraspecific interactions. *J. Mammal.* **100**, 1522–1532 (2019).
35. D. Oro, M. Genovart, G. Tavecchia, M. S. Fowler, A. Martínez-Abraín, Ecological and evolutionary implications of food subsidies from humans. *Ecol. Lett.* **16**, 1501–1514 (2013).
36. E. R. Pianka, Niche overlap and diffuse competition. *Proc. Natl. Acad. Sci. U.S.A.* **71**, 2141–2145 (1974).
37. T. J. Davies, S. Meiri, T. G. Barraclough, J. L. Gittleman, Species co-existence and character divergence across carnivores. *Ecol. Lett.* **10**, 146–152 (2007).
38. M. E. Gompper, Top carnivores in the suburbs? Ecological and conservation issues raised by the colonization of north-eastern North America by coyotes. *Bioscience* **52**, 185–190 (2002).
39. K. Crooks, M. Soulé, Mesopredator release and avifaunal extinctions in a fragmented system. *Nature* **199**, 563–566 (1999).
40. G. Roemer, M. Gompper, B. Van Valkenburgh, The ecological role of the mammalian mesocarnivore. *Bioscience* **59**, 165–173 (2009).
41. A. D. Rodewald, L. J. Kearns, D. P. Shustack, Anthropogenic resource subsidies decouple predator-prey relationships. *Ecol. Appl.* **21**, 936–943 (2011).
42. S. Warsen, "Evolving niche of coyotes in the Adirondack Mountains of New York: Long-term dietary trends and interspecific competition," MSc thesis, State University of New York, College of Environmental Science and Forestry, Syracuse, NY (2012).
43. S. A. Warsen, J. L. Frair, M. A. Teece, Isotopic investigation of niche partitioning among native carnivores and the non-native coyote (*Canis latrans*). *Isotopes Environ. Health Stud.* **50**, 414–424 (2014).
44. J. E. Carlson *et al.*, Potential role of prey in the recovery of American martens to Wisconsin. *J. Wildl. Manage.* **78**, 1499–1504 (2014).
45. P. J. Manlick, J. E. Woodford, B. Zuckerman, J. N. Pauli, Niche compression intensifies competition between reintroduced American martens (*Martes americana*) and fishers (*Pekania pennanti*). *J. Mammal.* **98**, 690–702 (2017).
46. D. M. Post, Using stable isotopes to estimate trophic position: Models, methods, and assumptions. *Ecology* **83**, 703–718 (2002).
47. S. D. Newsome, C. Martínez del Río, S. Bearhop, D. L. Phillips, A niche for isotopic ecology. *Front. Ecol. Environ.* **5**, 429–436 (2007).
48. C. A. Layman *et al.*, Applying stable isotopes to examine food-web structure: An overview of analytical tools. *Biol. Rev. Camb. Philos. Soc.* **87**, 545–562 (2012).
49. C. A. Layman, J. P. Quattrochi, C. M. Peyer, J. E. Allgeier, Niche width collapse in a resilient top predator following ecosystem fragmentation. *Ecol. Lett.* **10**, 937–944 (2007).
50. T. K. Pool *et al.*, Increased taxonomic and functional similarity does not increase the trophic similarity of communities. *Glob. Ecol. Biogeogr.* **25**, 46–54 (2016).
51. J. N. Pauli, M. Ben-David, S. Buskirk, J. DePue, W. Smith, An isotopic technique to mark mid-sized vertebrates non-invasively. *J. Zool. (Lond.)* **278**, 141–148 (2009).
52. S. Bearhop, C. E. Adams, S. Waldron, R. A. Fuller, H. Maceoed, Determining trophic niche width: A novel approach using stable isotope analysis. *J. Anim. Ecol.* **73**, 1007–1012 (2004).
53. G. D. Farquhar, J. R. Ehleringer, K. T. Hubick, Carbon isotope discrimination and photosynthesis. *Annu. Rev. Plant Physiol. Plant Mol. Biol.* **40**, 503–537 (1989).
54. A. H. Jahren, R. A. Kraft, Carbon and nitrogen stable isotopes in fast food: Signatures of corn and confinement. *Proc. Natl. Acad. Sci. U.S.A.* **105**, 17855–17860 (2008).
55. S. D. Newsome, K. Ralls, C. V. H. Job, M. L. Fogel, B. L. Cypher, Stable isotopes evaluate exploitation of anthropogenic foods by the endangered San Joaquin kit fox (*Vulpes macrotis mutica*). *J. Mammal.* **91**, 1313–1321 (2010).
56. B. C. Stock *et al.*, Analyzing mixing systems using a new generation of Bayesian tracer mixing models. *PeerJ* **6**, e5096 (2018).
57. A. L. Jackson, R. Inger, A. C. Parnell, S. Bearhop, Comparing isotopic niche widths among and within communities: SIBER—stable isotope Bayesian ellipses in R. *J. Anim. Ecol.* **80**, 595–602 (2011).
58. C. T. Darimont, P. C. Paquet, T. E. Reimchen, Landscape heterogeneity and marine subsidy generate extensive intrapopulation niche diversity in a large terrestrial vertebrate. *J. Anim. Ecol.* **78**, 126–133 (2009).
59. J. G. Way, A comparison of body mass of *Canis latrans* (coyotes) between Eastern and Western North America. *North-East. Nat.* **14**, 111–124 (2007).
60. R Core Team, *R: A Language and Environment for Statistical Computing*, (R Foundation for Statistical Computing, Vienna, Austria, 2019).
61. Stan Development Team, rstanarm: Bayesian applied regression modeling via Stan (R package version 2.13.1, 2016). <http://mc-stan.org>. Accessed 28 September 2020.
62. C. C. Monnahan, J. T. Thorson, T. A. Branch, Faster estimation of Bayesian models in ecology using Hamiltonian Monte Carlo. *Methods Ecol. Evol.* **8**, 339–348 (2017).
63. M. Smithson, J. Verkuilen, A better lemon squeezer? Maximum-likelihood regression with beta-distributed dependent variables. *Psychol. Methods* **11**, 54–71 (2006).
64. A. Vehtari, J. Gabry, Y. Yao, A. Gelman, loo: Efficient leave-one-out cross-validation and WAIC for Bayesian models (R package version 2.1.0, 2019). <https://cran.r-project.org/web/packages/loo/citation.html>. Accessed 28 September 2020.
65. J. Gabry, shinystan: Interactive visual and numerical diagnostics and posterior analysis for Bayesian models (R package version 2.4.0, 2017). <https://cran.r-project.org/web/packages/shinystan/index.html>. Accessed 28 September 2020.